ISIJ International, Vol. 42 (2002), No. 7, pp. 744–750

# Ultrafine Grain Structure through Dynamic Recrystallization for Type 304 Stainless Steel

Ilaria SALVATORI, Tadanobu INOUE[1)] and Kotobu NAGAI[1)]

Centro Sviluppo Materiali, Via di Castel Romano 100-00128 Roma, Italy. E-mail: i.salvatori@c-s-m.it
1) Metallurgical Processing Group, Steel Research Center, National Institute for Materials Science, Sengen, Tsukuba, 305-0047 Japan. E-mail: INOUE.Tadanobu@nims.go.jp

(*Received on November 21, 2001; accepted in final form on March 29, 2002*)

Ultrafine grain structure in the Type 304 austenitic stainless steel are pursed through dynamic recrystallization. The recrystallization behaviors are studied at various combinations of deformation temperatures and strain rates accompanying the higher strain under a plain strain compression. The effects of the strain, the strain rate and the deformation temperature are investigated, and the relationship between the deformation conditions and the dynamic recrystallized grain size is analyzed. The critical strain needed for the initiation of recrystallization increases with the Z–H parameter. Empirical equations concerning the critical strain and the dynamic recrystallized grain size are discussed, and processing parameter maps are proposed for the complete dynamic recrystallization.

KEY WORDS: austenitic stainless steel; ultrafine grain structure; heavy deformation; dynamic recrystallization.

## 1. Introduction

Ultra-refinement of grain structure exhibits a remarkable increase in its yield strength. The austenite to ferrite phase transformation can be utilized to obtain the ultrafine grain structure for ferritic steels but not for austenitic stainless steels. Hence recrystallization from heavily deformed austenite is an alternative method for the refinement of the austenitic steels.

The dynamic recrystallization that spontaneously occurs during the deformation at elevated temperatures appears to be a more suitable method from the engineering viewpoints than the static recrystallization that occurs during the heating at a higher temperature after the heavy deformation at an ambient temperature. This is because the flow stress required for the static recrystallization is higher with a more complicated processing route. Hence, the aim of the present study is to acquire an ultrafine grain structure for the Type 304L stainless steel through dynamic recrystallization.

Dynamic recrystallization (DRX) is a softening process. The phenomenon has been investigated in a large number of metals and alloys and for various deformation processes.[1–3)] The stress–strain ($\sigma/\varepsilon$) curve is believed to have a characteristic shape under the DRX. When the material is strain-hardened, the strain-hardening rate is positive throughout the deformation. However with the DRX, the strain-hardening rate diminishes markedly after a critical strain ($\varepsilon_c$), and the stress decreases gradually to a steady state value. In other words, the $\sigma/\varepsilon$ curve shows a stress peak at an early stage of the deformation. The curve is generally a single-peak type at the higher strain rates and of a multiple-peak type at the lower strain rates.

The equivalent effect of decreasing the strain rate and increasing the temperature on the DRX flow curve has been recognized under the high temperature deformation with a temperature corrected strain rate, Zener–Hollomon or Z–H parameter:[4)]

$$Z=\dot{\varepsilon}\exp(Q/RT) \quad \text{.....(1)}$$

where $\dot{\varepsilon}$ is the strain rate, $T$ is the absolute temperature, and $R$ is the gas constant. $Q$ denotes the apparent activation energy for softening during deformation and has the value of 410 kJ/mol for the 304 stainless steel.[5)]

The DRX starts to occur at a strain $\varepsilon_c$ that is lower than the peak strain ($\varepsilon_p$). $\varepsilon_c$ is usually between 60% and 80% $\varepsilon_p$ and is called the critical strain analogous to the static recrystallization. $\varepsilon_c$ depends on the material parameters (chemical composition, initial grain size) and the deformation conditions (strain path, deformation temperature, and strain rate), and it becomes larger with an increase in the initial grain size or the Z–H parameter.

The equilibrium grain size $D_s$ depends only on the Z–H parameter, $Z$. In general, $D_s$ is a power-law function of the steady-state flow stress $\sigma_s$.[6)] The relationship can be interpreted empirically as follows:

$$\sigma_s=kD_s^{-\alpha} \quad \text{.....(2)}$$

where $k$ is a constant and $\alpha$ is the coefficient between 0.66 and 0.8. Using the relation of $\sigma_s=AZ^m$, $D_s$ can be expressed in the following form:

$$D_s=k'Z^{-\beta} \quad \text{.....(3)}$$

where $k'$ is a constant and $\beta$ ($=m/\alpha$) is between 0.12 and 0.3.[6] This equation essentially states that the size of the new grains in the DRX is only controlled by the Z–H parameter.

Therefore, following aspects should be considered in the design of a deformation path for developing an ultrafine grain structure:

(a) A relatively large $Z$ is required according to Eq. (3). It is necessary to consider increasing the strain rate or decreasing the deformation temperature.
(b) Since a higher strain rate corresponds to a higher $\sigma_p$, a comparatively lower strain rate is preferred from the engineering aspects.
(c) Low deformation temperature and high strain rate results in a large $\varepsilon_c$. Therefore, a much heavier deformation is needed to promote dynamic recrystallization.

Accordingly, the processing conditions with various combinations of deformation temperatures and strain rates accompanying the higher strain were investigated under the plain strain condition in the present study.

## 2. Experimental Procedures

A Type 304 austenitic stainless steel (0.017% C, 0.58% Si, 1.05% Mn, 9.72% Ni, 18.47% Cr) that was hot rolled and annealed in the industrial mill was used for the present study. Samples were machined into rectangular shapes whose dimensions were 20 mm along the transverse direction, 18 mm along the rolling direction and 12 mm along the normal direction, as shown in **Fig. 1**.

A compression perpendicular to the rolling direction was performed on the samples using a plain strain compression machine (DSI, Gleeble 2000). Anvils with a width of 5 mm were made of tungsten carbide. Lubricants were not used at the contact surfaces between the anvils and the specimen so that a larger plastic strain could be introduced. It was possible to keep the specimen temperature and the strain rate constant during the compression test.[7]

Twenty different thermo-mechanical paths, consisting of compressions at various temperatures and various strain rates, were prepared. The deformation temperatures were 873 K, 1 023 K, 1 173 K, 1 273 K and 1 373 K, and the nominal strain rates were 0.01/s, 0.1/s, 1/s and 10/s. The nominal reduction for each sample was 75%, *i.e.* samples of 12 mm thickness were compressed to 3 mm one. Thermo-mechanical cycles consisted of heating to a deformation temperature at 5 K/s, holding for 60 s before compression at the temperature, compressing at a given nominal strain rate and eventually cooling by water. The as-received material had a mean grain size of approximately 32 $\mu$m. When the material was soaked for 60 s at various temperatures, grain growth was observed above 1 173 K and the grain size was 42±5, 70±5 and 106±5 $\mu$m at 1 173 K, 1 273 K and 1 373 K, respectively.

The metallographic analyses were carried out using optical and SEM microscopy, and an image analyzer was used to measure the grain size distribution. The grain size was measured by the intercept method.[8]

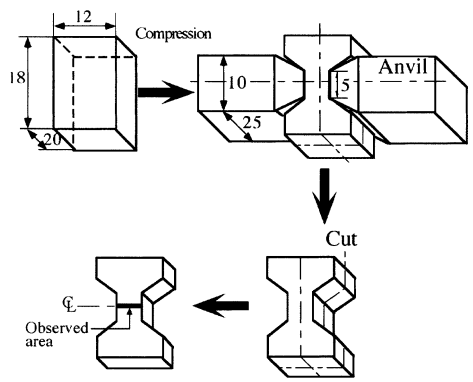


**Fig. 1.** Initial sample size and schematic drawing of the anvil compression.

## 3. Results

### 3.1. Stress–Strain Curves

Compression tests for the cylindrical samples were performed to understand the true stress–true strain behavior within a strain range of less than 0.8. **Figure 2** shows the true stress–true strain curves at the temperatures adopted in the present study at the strain rate of 0.01/s. Work hardening remained as the dominant process at 873 K, and the softening mechanism was not present within the tested strain range. At the temperatures of 1 023 K and higher, the softening mechanism was present, and the curve showed a typical shape for DRX. The peak stress decreased with an increase in temperature.

### 3.2. Compressive Strain Distribution inside the Sample

The strain in the compressed samples has a distribution with a maximum at the center of the sample.[7] The FE-analysis was used to evaluate the compressive strain distribution inside the samples introduced by the deformation. The contact condition between the anvils and the sample was adopted from the Coulomb odel with a friction coefficient of 0.3. Then the friction coefficient of 0.3 was determined by comparing the numerical result with the experimental measurement obtained from the sample with the screw.[7] **Figure 3** shows the calculated compressive strain distributions inside 75% compressed samples at various combinations of deformation temperatures and the nominal strain rates. The compressive strain distribution was mainly governed by the nominal reduction and was not affected much by the other parameters.

### 3.3. Microstructural Change by Compressive Strain

A compressed sample contains a wide range of strain distribution as shown in Fig. 3. Hence, the microstructural

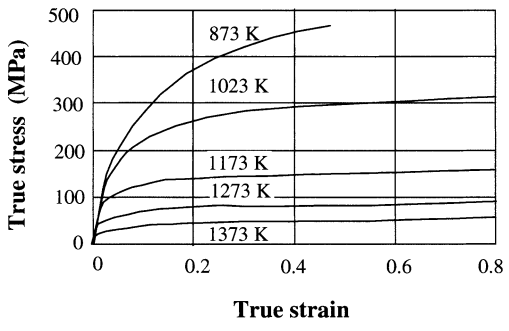


**Fig. 2.** True strees–true strain curves at different deformation temperatures when the strain rate is 0.01/s.

change along the centerline in the compressed samples has been analyzed with an optical microscope from one edge to the other with an interval of 100 $\mu$m.

**Figure 4**(a) represents the compressive strain and the strain rate distributions along the centerline for the 75% compressed sample at 1 173 K at a nominal strain rate of 0.1/s, and Figs. 4(b)–4(e) show the grain size distribution and the microstructures for the three sites. Since the strain has a distribution inside the samples, the strain rate also has a distribution. The local strain rate inside sample was determined as follows.

$$\dot{\varepsilon}=\frac{\varepsilon}{t} \quad \text{.....(4)}$$

where $\varepsilon$ is the compressive strain and $t$ is the deformation time. For example, in Fig. 4(a) the strain rate at the center of the specimen is about 0.22/s because $\varepsilon$ is 3.1 and $t$ is 13.86 s. The microstructures can be divided into three regions as shown in Fig. 4(b); a region with only initial grains (No DRX) near the sample surface (shown in Fig. 4(c)), a transition region consisting of some DRX ones together with the old grains (Partial DRX) (Fig. 4(d)), and a fully recrystallized region (Complete DRX) near the center of the sample (Fig. 4(e)). Furthermore, Fig. 4(b) shows that the DRX grain size becomes minimum at the center of the sample where the maximum strain and the strain rate were introduced.

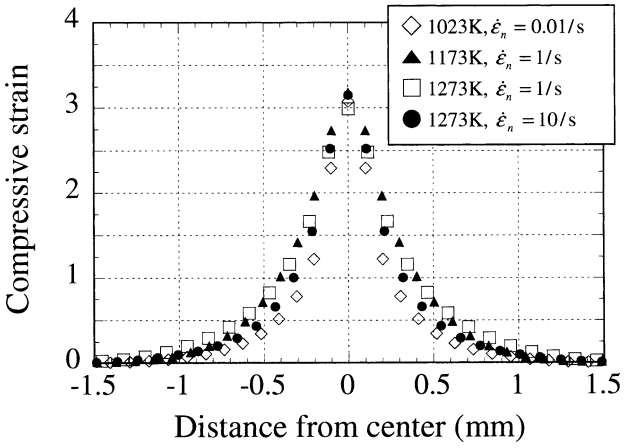


**Fig. 3.** Distribution of the compressive strain inside the sample, obtained by FE-analysis after a nominal reduction of 75%, where $\dot{\varepsilon}_n$ denotes the nominal strain rate.

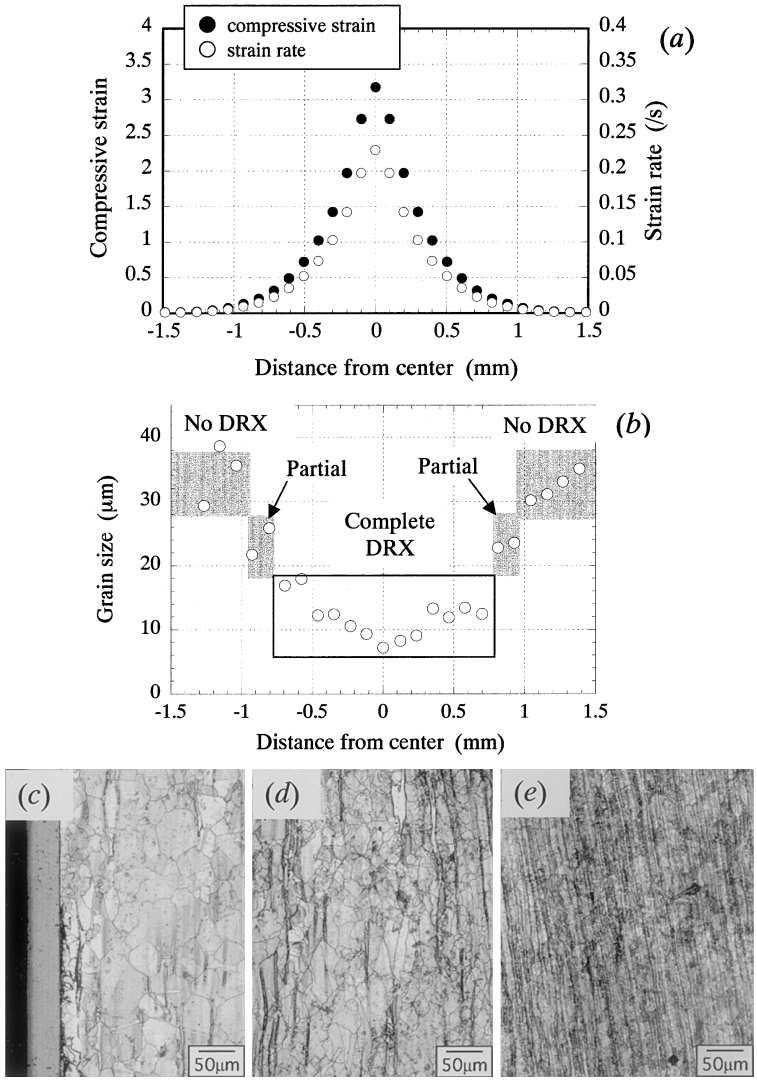


**Fig. 4.** (a), (b) Variations of the compressive strain, the strain rate and the grain size with distance from the sample edge, after a nominal reduction of 75% at a deformation temperature of 1 173 K and a nominal strain rate of 0.1/s. Microstructures when the distance from center is (c) −1.5, (d) −0.8 and (e) 0.

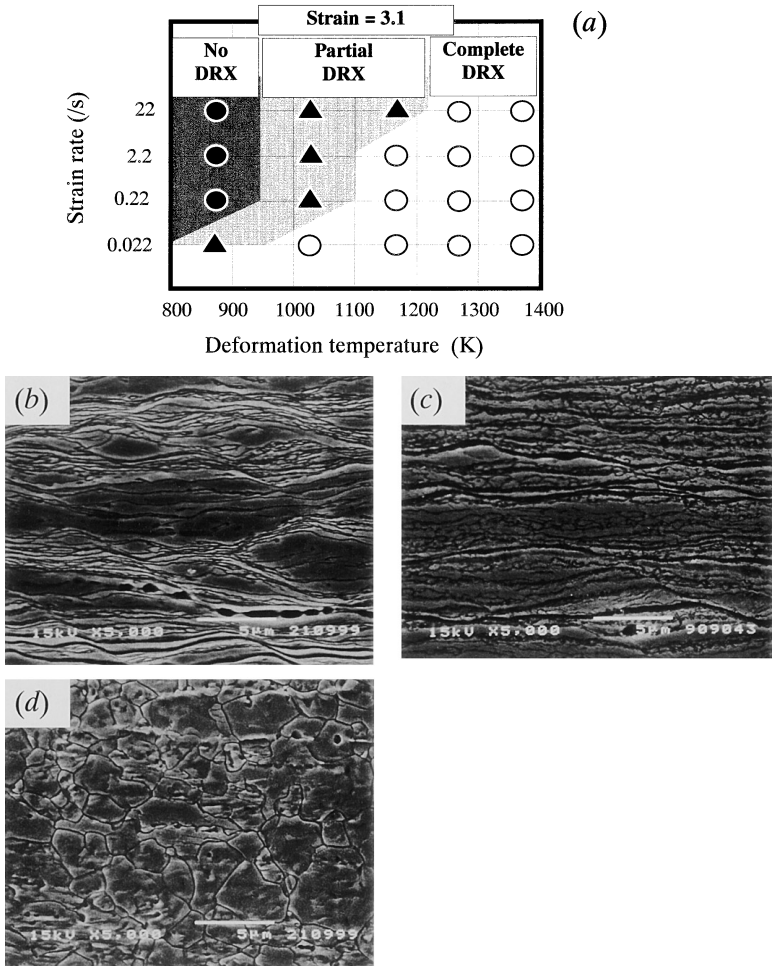


**Fig. 5.** (a) Mapping of DRX. (b) Microstructure (No DRX) at deformation temperature $T$=873 K and strain rate $\dot{\varepsilon}$=2.2/s. (c) Microstructure (Partial DRX) at $T$=1 023 K and $\dot{\varepsilon}$=22/s. (d) Microstructure (Complete DRX) at $T$=1 023 K and $\dot{\varepsilon}$=0.022/s.

### 3.4. Effect of Deformation Temperature and Strain Rate

To investigate the effect of the deformation temperature and the strain rate on the DRX behavior in the high compressive strain regime, the microstructure was observed and compared at the center of the samples compressed under various conditions. The largest compressive strain obtained was about 3.1 at the center of each sample.

**Figure 5** maps the recrystallization state at the center of each sample where the largest strain was obtained under various deformation temperatures and strain rates, and shows microstructures for three conditions; ($T$, $\dot{\varepsilon}$)=(873 K, 2.2/s), (1 023 K, 22/s) and (1 023 K, 0.022/s). According to the map in Fig. 5(a) the DRX tends to occur at a higher deformation temperature or at a lower strain rate. Note that the complete DRX occurs even at low deformation temperatures when the strain rate is low (see the point of $T$= 1 023 K and $\dot{\varepsilon}$=0.022/s). **Figure 6** is a TEM image of the new grains that appeared at the center of the compressed sample at $T$=1 023 K and $\dot{\varepsilon}$=0.022/s. Although the misorientation was not determined, many crystallographic orientations appear in the narrow area with a large number of new grains and the dislocation density is not high in the interior, hence the new grains are believed to be the DRX grains

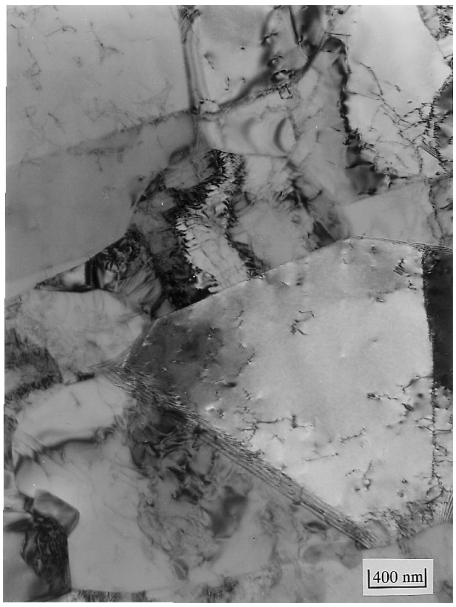


**Fig. 6.** TEM image of the newly formed small grains after DRX.

**Figure 7** illustrates the grain size at various deformation temperatures and strain rates only for the complete DRX samples. The DRX grain size decreases with a decrease in the deformation temperature or with an increase in the strain rate. The smallest grain size obtained in the present

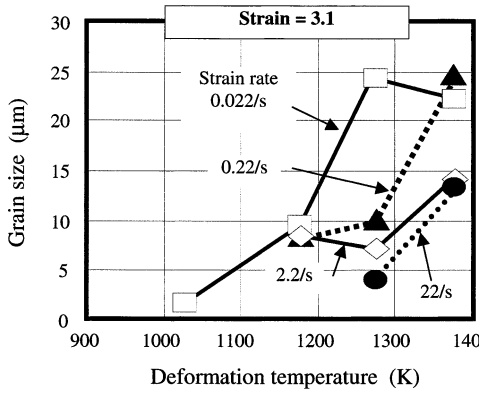


**Fig. 7.** Grain size *versus* deformation temperature and strain rate measured at the center of the sample where the strain is 3.1.

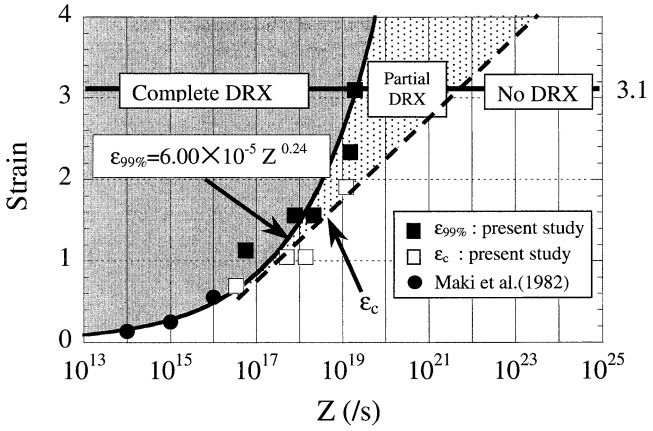


**Fig. 9.** Relation between the critical strain and the Zener–Hollomon parameter.

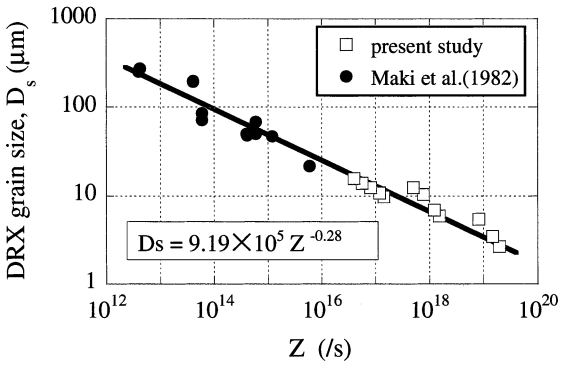


**Fig. 8.** DRX grain size *versus* the Zener–Hollomon parameter.

study is about 2.5 $\mu$m when the strain rate is 0.022/s, and the deformation temperature is 1 023 K. It is interesting that at 1 023 K, the complete DRX occurred only at the lowest strain rate.

As a result, it is possible to make a fine grained structure for the Type 304 at a low deformation temperature and at a low strain rate in a heavy strain regime.

## 4. Discussion

### 4.1. Controlling Factor of DRX Grain Size

As mentioned earlier, the main factor controlling the DRX grain size, $D_s$, is believed to be the Z–H parameter. The initial grain size, $D_o$, does not have much significance. Hence, we compare the present data with the data provided by Maki *et al.*[10] Their $D_o$ was between 76 and 250 $\mu$m and ours was about 30 $\mu$m. **Figure 8** rearranges the $D_s$ data as a function of the Z–H parameter. The open squares represent the data from the present study, and the solid circles from that of Maki *et al*. All the data lie on the same line which can be described in the form of Eq. (3). Here the exponent $\beta$ is 0.28, which is within the range reported in the literature.[6]

This analysis suggests that the DRX in the ultrafine grain range might be based on the same DRX phenomenon with that of conventional grain size.

Furthermore, Fig. 8 shows that the smallest DRX grain size (2.5 $\mu$m) that was obtained at the lowest strain rate (0.022/s) at the lowest deformation temperature (1 023 K) within the scope of the present study is reasonable. From this aspect, a more essential issue is to understand why the DRX did not occur at the higher strain rates at that deformation temperature.

### 4.2. Strain Required for DRX

**Figure 9** shows the strains required for the initiation ($\varepsilon_c$) and the 99% completion ($\varepsilon_{99\%}$) of the DRX as a function of the Z–H parameter. Here, the plotted data were measured for the Z–H parameter from the relation between the strain distribution and the microstructural change along the centerline in the compressed samples that are shown in Figs. 4(a) and 4(b). Some data by Maki *et al.* were also plotted in Fig. 9.

In Fig. 9, the equation of $\varepsilon_{99\%}$ as a function of $Z$ obtained by fitting all the data is shown. The equation is believed to be equivalent to the relationship between the recrystallized grain size and the Hollomon parameter (Sakui 1977).[11]

$$\varepsilon_{99\%}=AZ_s^{\gamma} \quad \text{.....(5)}$$

Here the exponent $\gamma$ is 0.24, which is comparable to the exponent $\beta$ (0.284) in Eq. (3).

It should be noted that heavier strain is required to initiate or complete DRX when Z–H parameter become higher.

### 4.3. Deformation Temperature–Strain Rate Map for DRX

Equations (3) and (5) can be combined into Eq. (6):

$$\varepsilon_{99\%}=BD_s^{\eta} \quad \text{.....(6)}$$

Here the exponent $\eta$ is $-0.86$, and this relation is shown in **Fig. 10**. Equation (6) gives the smallest strain to the complete DRX with a given DRX grain size in the one-pass compression. A coarser grain size that is larger than 5 $\mu$m needs a strain that is smaller than 2. However, a finer grain size that is smaller than 1 $\mu$m needs a heavy strain that is larger than 8.

The processing factors of the deformation temperature and the strain rate for the complete DRX can also be mapped according to the equations obtained in the present study as shown in **Figs. 11** and **12**. Figures 11(a) and 11(b) show the boundary of the complete DRX region for the given strain 3.1 in the present study and for other values of strains, respectively. We can obtain the complete DRX by

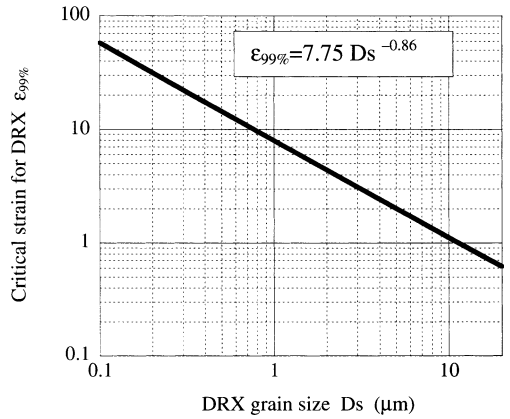


**Fig. 10.** Minimum strain required to obtain a grain DRX grain size.

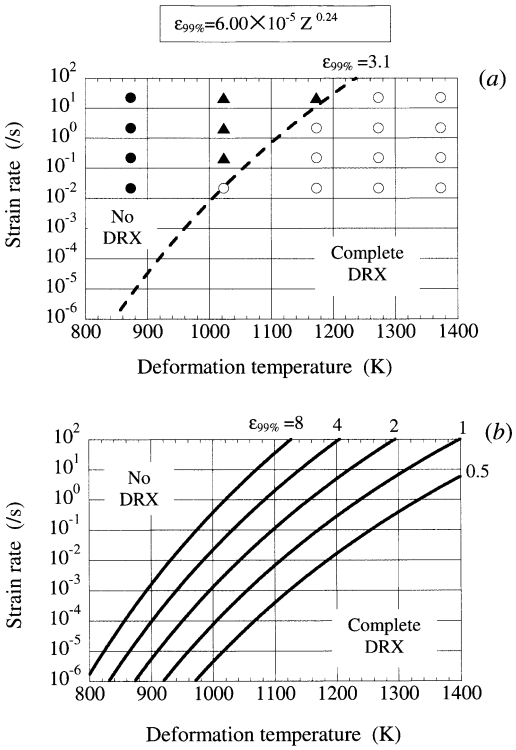


**Fig. 11.** Curves showing the boundary for a complete DRX condition of deformation temperature and strain rate for the given strains. (a) Curve of the boundary for the maximum strain of 3.1 with the results shown in Fig. 5(a). (b) Curves of the boundary for the various strains.

using the conditions under the curve for a given strain. Figure 12 shows the curve for a given DRX grain size when the complete DRX can be obtained. Therefore, we can figure out the obtainable DRX grain sizes, and the corresponding deformation temperature–strain rate conditions using these figures. For example, when the strain is 3.1, Fig. 12(b) shows the region where the DRX grain sizes that are larger than 2.5 $\mu$m can be obtained, and gives the combination of the deformation temperature and the strain rate. At a given deformation temperature, the higher strain rates produces a finer DRX grain size. At a given strain rate, the lower deformation temperature produces a finer DRX grain size. However, the strain rate range that achieves the DRX shifts to a lower band or the maximum strain rate decreases

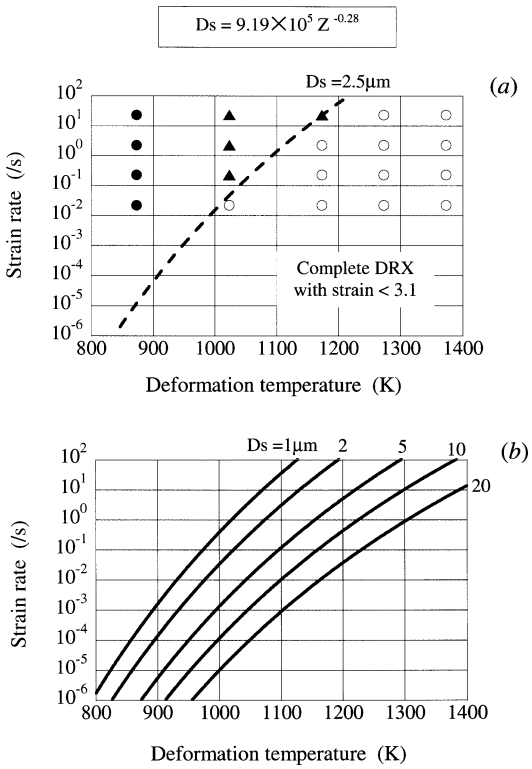


**Fig. 12.** Curves for the gicen DRX grain sizes in the deformation temperature–strain rate map. (a) Curve of the smallest DRX grain size 2.5 $\mu$m obtained in the present study. (b) Curves of the given DRX grain sizes.

with a lower deformation temperature.

## 5. Conclusions

Ultrafine grain structure in the Type 304 stainless steel has been pursued through dynamic recrystallization under a plain strain condition. The processing conditions with a lower deformation temperature and a lower strain rate in the strain range up to 3.1 were investigated.

(1) A grain size of 2.5 $\mu$m was obtained with the condition of a low deformation temperature and a low strain rate when the strain was 3.1.

(2) The grain size as well as the critical strain that was necessary for completing the dynamic recrystallization was determined as a function of the Z–H parameter.

(3) Processing parameter maps were proposed for the complete dynamic recrystallization.

**Acknowledgements**

I, I.Salvatori, would like to thank Dr. Okada, general director of NRIM, for accepting me as a Science and Technology Fellow, and Prof. T. Maki for very fruitful discussions on dynamic recrystallization.

## REFERENCES

1) T. Sakai and J. J. Jonas: *Acta Metall.*, **32A** (1984), 189.
2) H. J. McQueen, E. Evangelista and N. Ryan: Recrystallization in Metallic Materials, ed. by T. Chandra, TMS-AIME, Warrendale, PA, (1990), 89.
3) F. Montheillet and J. J. Jonas: *Encyclopedia of Applied Physics*, **16** (1956), 205.
4) C. Zener and J. H. Hollomon: *Trans. Am. Soc. Met.*, **33** (1944), 163.

5) D. J. Towle and T. Gladman: *Met. Sci*., **13** (1979), 246.
6) B. Derby: *Acta Metall*., **39** (1991), 959.
7) T. Inoue, S. Torizuka, K. Nagai, K. Tsuzaki and T. Ohashi: *Mater. Sci. Technol*., **17** (2001), 1580.
8) ASTM Standard E112, Metals test methods and analytical procedures, Philadelphia, PA, USA, (2000).
9) ABAQUS/Explicit ver. 5.8, User's manual, Hibbit, Karlsson & Sorensen, Inc., USA, (1998).
10) T. Maki, K. Akasaka, K. Okuno and I. Tamura: *Trans*. *Iron Steel Inst. Jpn*., **22** (1982), 253.
11) S. Sakui, T. Sakai and K. Takeishi: *Trans*. *Iron Steel Inst. Jpn.*, **17** (1977), 718.